Free-Bending Fatigue Life Estimation of Cables at Points of Fixity

By Mohammed Raoof[1]

Abstract: The shortcomings of the traditional design approaches based on the extreme fiber (in terms of simple beam theory) direct wire stresses as the factor controlling strand restrained bending fatigue performance, have been resolved. A new parameter has been proposed, which largely overcomes these limitations and is capable of predicting free-bending fatigue life of axially preloaded spiral strands clamped at the end. The model explains some experimental observations, which have found the initial wire fractures at the fixed ends being invariably located at the so-called neutral axis rather than (as might be expected), at the extreme fiber position. The theory attributes the occurrence of interwire-interlayer fractures to the fretting fatigue phenomenon, and takes interwire friction fully into account. The new model is found to give very encouraging correlations with available experimental fatigue data on some substantial spiral strands. The theory also demonstrates the possibility of substantial reductions in sheathed spiral strand free-bending fatigue life in deep-water applications. In the past, such effects were invariably ignored in the design of mooring systems in, say, deep-water guyed-tower platform applications. By employing practical simplifying assumptions, a similar parameter for estimating the free-bending fatigue life of multistrand ropes, in the vicinity of end terminations, has also been proposed.

Introduction

Free-bending fatigue problems are a source of concern (and not infrequent failures) in structures ranging from suspension and cable-stayed bridge hangers and the stays for guyed masts to electromechanical cables, where fatigue failures near partially restrained terminations are not uncommon. These failures are caused by, for example, aero- or hydrodynamic loading.

In the early 1980s, a report for the U.K. Department of Energy (Webster et al. 1982) identified an urgent need for a better understanding of the axial and free-bending performance of large diameter (e.g., 127-mm outer diameter (OD) or larger) strands, for which there appeared to be very little available information.

In a series of recent publications [e.g., Raoof and Hobbs (1984, 1988, 1989), and Raoof (1989, 1990a–e, 1992)], the present writer and his associates have put substantial effort into assessing the contact forces and the associated relative displacements between wires, taking full account of frictional effects, in large spiral strands. It is now well established that a thorough understanding of the pattern of interwire-interlayer contact forces and associated fretting movements is central to a fundamental understanding of spiral strand fatigue performance.

For the present purposes, much attention will be devoted to the free-bending fatigue life prediction of axially preloaded and large-diameter spiral strands. Such information should prove particularly useful during the preliminary phases of design, and is believed to be of value for achieving an optimal design for a particular application.

---

[1]Bridon Reader, Civ. and Struct. Engrg. Dept., South Bank University, Wandsworth Road, London SW8 2JZ, United Kingdom.

Note. Discussion open until February 1, 1993. To extend the closing date one month, a written request must be filed with the ASCE Manager of Journals. The manuscript for this paper was submitted for review and possible publication on September 10, 1991. This paper is part of the *Journal of Engineering Mechanics*, Vol. 118, No. 9, September, 1992. ©ASCE, ISSN 0733-9399/92/0009-1747/$1.00 + $.15 per page. Paper No. 2263.

It is perhaps worth noting that despite the efforts of research workers dating back to the early years of this century, little light has been cast on the free-bending behavior of helically laid cables taking interwire-interlayer friction into account (Raoof and Hobbs 1984). An understanding of this problem is central to the development of interwire fretting fatigue models suitable for free-bending fatigue life prediction for strands (Raoof 1989). The literature on free bending of cable has already been reviewed elsewhere (Raoof and Hobbs 1984; Raoof, 1989). Perhaps, it will suffice to mention some fairly recent attempts by various authors [e.g., Nowak (1974), Costello and Butson (1982), Knapp (1988)] who have invariably ignored the presence of interwire-interlayer friction and attempted to estimate the magnitude of wire direct stresses in spiral strands under uniform bending to a constant radius of curvature away from points of fixity, such as, for example, end terminations. Recent work by Raoof and Huang (1991), however, has demonstrated the major shortcoming of such frictionless theories. They have shown that inclusion of interwire friction does, at least in the vicinity of end terminations, lead to a very substantial increase in the values of calculated direct stresses in wires under bending, when compared with the corresponding estimates based on frictionless theories. These frictionless models treat the individual wires as helical rods with much emphasis on the bending and torsion of the individual elements: these are unlikely to be of any significance in large-diameter and multilayered strands, for which the present model is developed.

In the related field of overhead transmission lines, several approaches have been proposed for obtaining estimates of maximum direct strains: limiting such strains is generally believed to minimize potential free-bending fatigue problems at the end terminations (Poffenberger and Swart 1965; "Standardization" 1965; Richardson 1989). In the field of structures, in line with the traditional maximum stress approaches, Hobbs and Smith (1983) used the fatigue data reported by Hobbs and Ghavami (1982) on 7.9-m-long and 39-mm-OD spiral strand to calibrate their model. However, in their free-bending fatigue tests on axially preloaded spiral strands, Hobbs and Ghavami found the first wire fractures invariably occurred at the neutral axis (in terms of simple beam bending theory) rather than (as might be expected) at the extreme fiber position. The subsequently developed theoretical models (Raoof and Hobbs 1984, Raoof 1990b) attributed the occurrence of first wire fractures in the vicinity of neutral axis to the presence of rather significant levels of interwire fretting displacements, which were theoretically found to be greatest at the neutral axis and were shown to gradually diminish in magnitude as one approached the so-called extreme fiber position. This is in direct contrast to the general approach, currently adopted by practicing engineers, who invariably aim at limiting the calculated (or measured) direct stresses (or strains) in order to control (or eliminate) the potential free-bending fatigue problems.

In a recent paper, Raoof (1989) produced substantial experimental support for these theoretical findings (Raoof 1990b): Interlayer slippage was shown experimentally to be greatest at the neutral axis. Raoof (1989) also briefly outlined the basic nature of a newly developed contact stress-slip parameter, which appeared to successfully predict the free-bending fatigue life of a number of axially preloaded spiral strands, although, due to space limitation, full details of the theoretical model were not reported. Most importantly, it was argued that this new parameter took interwire-interlayer fretting fatigue phenomenon fully into account.

Objectives

The purpose of this paper is to present full details of a theoretical model for predicting the magnitude of contact stress-slip parameter for any axially preloaded spiral strand construction. Moreover, it will be shown that with one reasonable simplifying assumption, closed-form solutions can be obtained for Raoof's (1990b) differential equation, whose solution leads to estimates of the magnitude of maximum interwire slippage, which is an important component of the contact stress-slip parameter. In Raoof's previous paper (1990b), a standard numerical computer package was used for solving the nonlinear differential equation. It will also be demonstrated that a similar parameter may prove of value when addressing the free-bending fatigue life prediction for multistrand ropes. Finally, it will be shown that, in the case of sheathed spiral strands used in deep-water platform applications, the rather significant levels of external hydrostatic pressure on such a sealed construction can lead to significant reductions in the calculated free-bending fatigue life of the axially preloaded strands. This may be of practical significance in relation to the integrity of the end terminations at the sea bottom.

Theory

Following experimental observations (Raoof 1989) for the restrained bending of an axially preloaded, multilayered strand at a fixed end, the spiral strand may be modeled as single layer of wires over a rigid core undergoing plane-section bending (Raoof 1990b).

Wire axial strain, ε^{l}, due to bending of a single-layered and axially preloaded spiral strand undergoing bending to a constant radius of curvature, ρ, may be calculated using an extended version of Lutchansky's model (1969). Lutchansky assumes that the change in the axial tension of a helical wire with strand bent to a constant radius of curvature, ρ, is balanced by the external interaction shear force (Fig. 1), so that

$$dN = K_1(u - u^p)\, ds_c \quad \text{(1)}$$

where N = wire axial tension; K_1 = interwire-interlayer shear stiffness; u = local axial wire displacement; and u^p = underlying core displacement. Using (1), Lutchansky derived a differential equation in terms of wire displacement, u, as

$$\frac{d^2u}{ds_c^2} - \frac{K_1 u}{AE} = -\frac{K_1 U}{AE}(\sin\theta - \sin\theta_0) \quad \text{(2)}$$

where θ = the polar angle of the helix measured from the point at which the helix first crosses the extreme fiber position of the bent cylinder. θ_0 denotes the helix polar angle at which the toroidal section starts; A = wire cross-section area; E = Young's modulus; and $c = \sqrt{(r_1 - r_w^2) + k^2}$,with k = pitch of the helix divided by 2π; r_1 = helix radius; and r_w = wire radius. The parameter U' is given as

$$U' = \frac{k^2(r_1 - r_w)}{\rho c} \quad \text{(3)}$$

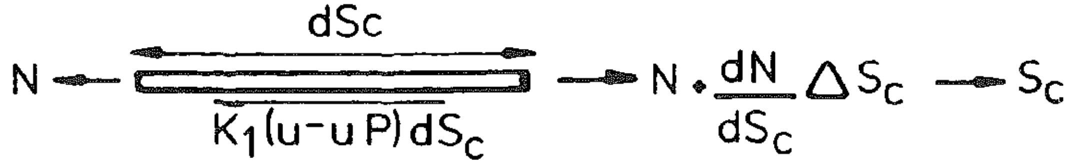

FIG. 1. Forces on Wire Element

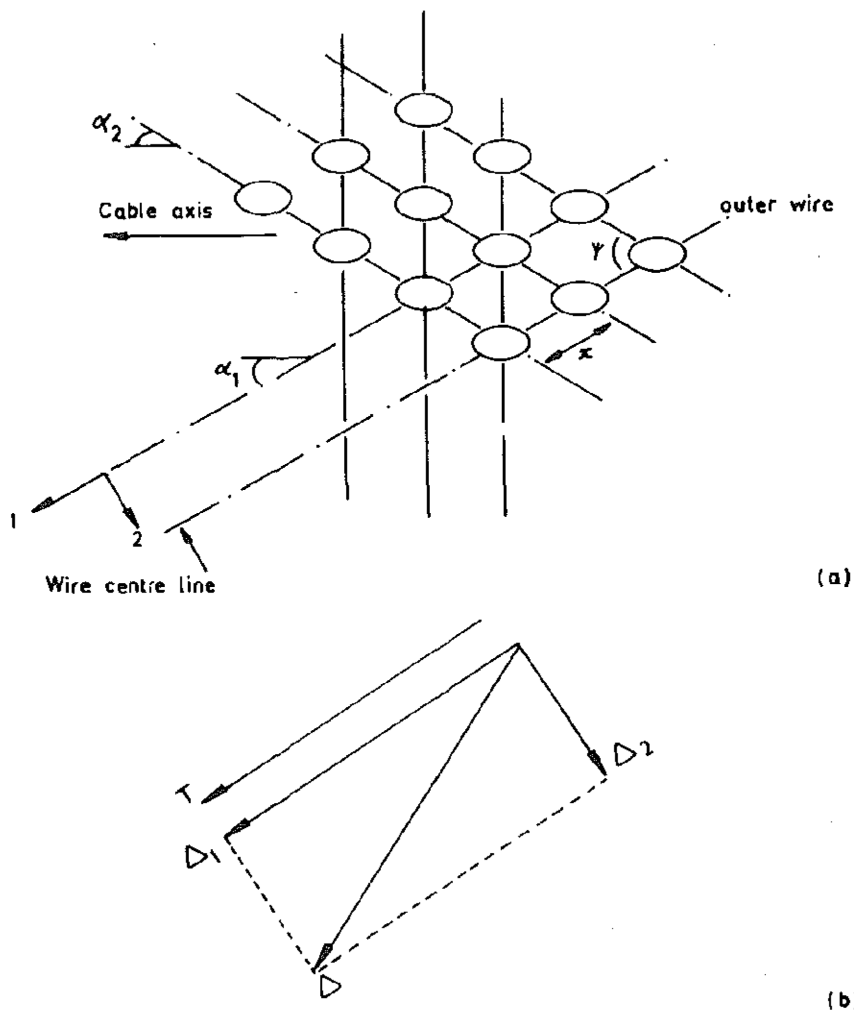

FIG. 2. Pattern of Interlayer Contact Patches

and the plane section displacement taking the path of the helix on the surface of the toroid, u^p, is (Lutchansky 1969)

$$u^p = U'(\sin\theta - \sin\theta_0) \quad \ldots\ldots (4)$$

For a strand rigidly clamped at one end and bent to a constant radius of curvature, ρ, (2) may (for a constant value of K_1) be solved with the appropriate boundary conditions to give

$$\frac{du}{ds_c} = \frac{k^2(r_1 - r_w)K_1}{\rho(AE - c^2K_1)}\left(\frac{1}{c}\sqrt{\frac{AE}{K_1}}\, e^{\sqrt{K_1/AE}(\theta_0-\theta)}\cos\theta_0 + \sin\theta\right) \quad \ldots\ldots (5)$$

For a constant (no-slip) value of shear stiffness, K_1, Lutchansky used (5) to show that the highest strain, $(du/ds_c)_{\max}$, occurring at the clamp is in the wire with

$$\theta_0^{max} = -\tan^{-1}\left(\frac{1}{c}\sqrt{\frac{AE}{K_1}}\right) \quad (6)$$

Determination of Stiffness Factor, K_1

In a cross-laid construction, the outer-layer wires touch the underlying core at a number of isolated contact patches in a trellis pattern [Fig. 2(*a*)]. It is further assumed that the number of such projections is large enough that any local effects can be ignored. This is analogous to the concept of contact between two bearing surfaces occurring at the tips of their surface asperities. Herzian normal contact theory may be used to compute the sizes of the individual elliptical contact patches whose semimajor and minor axes are a and b (Raoof 1990b). This, coupled with the work of Vermeulen and Johnson (1964), provides an analytical model that gives the shear stiffness of the individual contact patches along their principal axes. Determination of the overall shear stiffness of a large number of isolated ellipses along the individual wire axes will then follow, using recent formulations reported by Raoof and Hobbs (1989). Full details for the most general case of anisotropic contact is given by Raoof (1990b). However, in what follows, some reasonable simplifications will be made regarding the theoretical formulations that lead to a considerable saving with respect to computational efforts required to solve the nonlinear version of differential (2). It must be noted that the proposed simplifications are believed to be compatible with the other assumptions inherent in the model, such as uncertainties associated with the pattern of interwire-interlayer contact forces, P_R, in the vicinity of the socket, and more importantly, the uncertainties associated with the assumed value of the coefficient of friction, μ. Strictly speaking, due to the orthotropic nature of the contact problem, the direction of the resultant shear displacement, Δ, does not coincide with the direction of the applied shear force [Fig. 2(*b*)]. The displacement Δ can then be resolved into two components along the first and second directions (1 and 2). A simple manipulation of the results by Vermeulen and Johnson (1964) for the compliance of two nonspherical bodies in contact along one of the principal axes of their elliptic contact area gives

$$\frac{d\delta_l}{dT} = \frac{\Gamma\left(\frac{a}{b}\right)}{\pi b G}\left(1 - \frac{\delta_l}{\delta_{l\max}}\right)^{-1/2} \quad (7)$$

where

$$G = \frac{E}{2(1 + \nu)} \quad (8a)$$

and

$$\delta_{l\max} = \frac{3\mu P_R(1 + \nu)}{\pi b E}\Gamma\left(\frac{a}{b}\right) \quad (8b)$$

and

$$\Gamma\left(\frac{a}{b}\right) = \begin{cases} K - \nu D & a < b \\ \pi \dfrac{(2 - \nu)}{4} & a = b \\ \dfrac{b}{a}(K - \nu B) & a > b \end{cases} \qquad (9)$$

In (9), K, B, and D are the complete elliptic integrals defined and tabulated by Janke and Emde (1945) in terms of a modulus

$$k_1^2 = \frac{a^2}{b^2} - 1 \quad \text{for} \quad a < b \qquad (10a)$$

and

$$k_1^2 = 1 - \frac{b^2}{a^2} \quad \text{for} \quad a < b \qquad (10b)$$

The tangential force, T, is directed along the principal axis of the ellipse of contact, and the semi-axis a, corresponds to the axis parallel to T. The other semi-axis is denoted by b. E = Young's modulus; ν = Poisson ratio; μ = coefficient of friction; and P_R = normal force on the contact patch. The magnitude of P_R may be obtained by a method suggested by Raoof and Hobbs (1988), while the sizes a and b may be calculated following the procedure reported by Raoof (1990b).

The nonlinear version of (2) with proper (variable) K_1 values may be solved by the method suggested by Raoof (1990b), who took the anisotropic nature of interlayer contact fully into account. However, the following simple observations will enable one to obtain closed from solutions for the magnitude of interwire-interlayer slippage, $u - u^p$, with one simplifying assumption. Following results from an extensive set of parametric studies on a number of strands with widely different construction details, it has been found that, at least for the practical ranges of manufacturers' constructional limits for lay angle and wire or cable diameters, the influence of the anisotropy on the results for K_1 value in (2) may, for all practical purposes, be reasonably ignored. Moreover, for the practical (working) ranges of strand mean axial loads, it has invariably been found that the transition from no-slip to full-slip interlayer slippage in the vicinity of a socket does occur at rather large levels of radii of curvature (i.e., small values of interlayer slippage) at the termination. The effect of the value of K_1 on the magnitude of interlayer slippage has invariably been found to be very small.

Close examination of (7) and (8b) indicate that gross slippage occurs when $T = \mu P_R$ with the displacement at the onset of gross slippage, $\delta_{l\max}$, given by (8b). However, for the no-slip case, the initial tangent to the T versus δ_l curve for an isolated contact patch is given by

$$\delta_l = \left(\frac{d\delta_l}{dT}\right)_{T=0} \cdot T \qquad (11)$$

thus, when $T = \mu P_R$, we have

$$\delta_{li} = \frac{2\mu P_R(1 + \nu)}{\pi b E} \Gamma\left(\frac{a}{b}\right) \qquad (12a)$$

$$\delta_{li} = \frac{2}{3}\,\delta_{l\max} \quad \text{(12b)}$$

It is concluded that the displacement at the onset of gross slippage, $\delta_{l\max}$, is 1.5 times greater than the elastic displacement calculated on the no-slip assumption. Bearing in mind the previous comments regarding the influence of the exact value of K_1 on the calculated values of interlayer slippage, δ_l, it may reasonably be assumed that for $u - u^p = \delta_l < \delta_{li}$, the no-slip value of shear stiffness, K_{1n}, may be used, that is

$$K_{1n} = \frac{\mu P_R}{x\delta_{li}} \quad \text{(13)}$$

where x = spacing between the contact patches along the outer wire, as given by (Phillips et al. 1980)

$$x = \frac{2\pi r}{n_2}\,\frac{\cos \alpha_2}{\sin(\alpha_1 - \alpha_2)} \quad \text{(14)}$$

where α_1 and α_2 = lay angles in first (outer) and second layers, respectively; n_2 denotes the number of wires in the second (penultimate) layer; $r = r_1 - D/2$, where r_1 = helix radius in outer layer; and D = wire diameter in that layer. If $u - u^p = \delta_l \geq \delta_{li}$, then the full-slip shear stiffness, K_{1f}, for the nonlinear version of (2) is given by

$$K_{1f} = \frac{\mu P_R}{(u - u^p)x} \quad \text{(15)}$$

Estimation of Interwire-Interlayer Slippage

Using the bilinear relationship between T and δ_l, the value of interwire-interlayer slippage in the vicinity of the neutral axis, over a trellis contact patch at a distance equal to trellis contact patch spacing, x, from the ideal fixed end, may be obtained from

$$U = u - u^p \quad \text{(16)}$$

where u^p is given by (4) with

$$\theta_0 = \theta_0^{\max} - \frac{\pi}{2} \quad \text{(17a)}$$

and

$$\theta = -\left(|\theta_0| - \frac{x}{c}\right) \quad \text{(17b)}$$

In (17a, b) $\theta_0^{\max}$ is given by (6) and θ_0 defines the polar angle at the fixed end for the critical wire experiencing maximum slippage. Following Lutchansky's (1969) definition, θ_0 is always negative. The parameter θ, on the other hand, gives the polar angle of the center of critical trellis contact patch at a distance x along the wire from the ideal fixed end.

The magnitude of u, depends on the value of the shear stiffness and may be calculated as follows,

1. For the no-slip case (i.e., $\delta_l \leq 2/3\delta_{l\max}$), the solution to the differential equation [(2)] with appropriate boundary conditions is (Lutchansky 1969)

$$u = \frac{U' \sin \theta_0}{1 + \frac{c^2 K_{1n}}{AE}} \cdot \exp \left[\sqrt{\frac{K_{1n}}{AE}} c(\theta_0 - \theta) \right]$$

$$+ U' \left[\frac{K_{1n} c^2}{AE + c^2 K_{1n}} \sin \theta - \sin \theta_0 \right] \quad \text{(18)}$$

where the symbols are as defined previously.

2. For the full-slip case (i.e., $\delta_l > 2/3\ \delta_{l\max}$), the numerical results based on solutions of the nonlinear version of (2) with variable (fully nonlinear) K_1-values, covering a wide range of strand (and wire) diameters and lay angles, strongly suggest that the value of u in (16) may be ignored, for all practical purposes, since it is insignificant in relation to the magnitude of the parameter u^p. This is particularly true when dealing with large-diameter (greater than 15-mm OD, say) strands, which are the type of strands for which Raoof's (1990b) theoretical model was originally developed.

It must be noted that, the solution to case 1 with $\delta = 2/3\delta_{l\max}$ may prove useful in identifying a threshold value for the radius of curvature, ρ (implicit in the parameter U' as defined by (3), for which full sliding, and hence fretting, can become significant. It should, therefore, prove of some value, when addressing the possible presence of a free-bending endurance limit, below which no significant damage is likely to occur. Finally, the preceding developments ignore the component of interwire slippage due to the bending of the individual wires about their own axes. This effect, however, is of little significance in relation to large-diameter strands (with very small wire-to-strand-diameter ratios) considered in the present paper (Raoof and Huang 1992).

Calculation of Maximum Tensile Stress

The magnitude of the alternating tensile stress, σ_x, at the trailing edge of the elliptic trellis contact patch, may be obtained by a simple manipulation of formulations developed by Vermeulen and Johnson (1964), where the final result for our present purposes is

$$\sigma_x = \frac{3\mu P_R}{\pi a^2} (D + C\nu) \quad \text{(19)}$$

where μ = interwire coefficient of friction; P_R = normal contact force on the trellis contact patch; a = semimajor axis of the elliptic contact patch; ν = Poisson ratio; and C and D = elliptic integrals, defined as

$$C = \frac{(2D - K)}{k_1^2} \quad \text{(20a)}$$

$$D = \frac{(K - E)}{k_1^2} \quad \text{(20b)}$$

where (Jehnke and Emde 1945)

$$E = \int_0^{\pi/2} \sqrt{1 - k_1^2 \sin^2 \theta}\, d\theta \quad \text{(20c)}$$

and

$$K = \int_0^{\pi/2} \frac{1}{\sqrt{1 - k_1^2 \sin^2\theta}}\, d\theta \quad \text{(20}d\text{)}$$

with

$$k_1^2 = 1 - \frac{b^2}{a^2} \quad \text{(20}e\text{)}$$

In the preceding, b = semiminor axis of the elliptical trellis contact patch, whose major-axis half-width is a.

Johnson and O'Connor (1963), among others, have emphasized the importance of the alternating tensile stresses at the edge of the contact patch, on which is superimposed a local state of steady tensile stress due to the Hertzian normal pressure, as a possible cause of fretting fatigue crack initiation.

Contact Stress-Slip Parameter

For an axially preloaded spiral strand experiencing a maximum radius of curvature, ρ, at the fixed end, the proposed formulations lead to estimates of maximum interwire slippage, U, and maximum value of the alternating tensile stress at the trailing edge of the trellis contact patch, σ_x. The contact stress-slip parameter, S, may then be defined as

$$S = \frac{U\sigma_x}{x} \quad (21)$$

It is encouraging that the use of this parameter makes it possible to draw a single curve through the experimental data of several realistic multi-layered strands with different makeup (Fig. 3), i.e., this parameter has a predictive value. This may be contrasted with the traditional method of presenting data by plotting the calculated (or measured) maximum extreme fiber wire stresses against fatigue life, where the ability to sketch well-separated curves through the data points of each individual strand makeup represents a weak correlation.

Calculation of the newly developed parameter is as follows.

1. Calculate $(EI)_{\mathrm{eff}}$ by the method suggested by Raoof (1989), and hence, for a given mean axial load, obtain the magnitude of the maximum radius of curvature at the fixed end.
2. Use the method developed by Raoof and Hobbs (1988) to calculate the magnitude of the normal force on the trellis contact patch, P_R, between the outer and penultimate layers (layers one and two, respectively).
3. Calculate the sizes of semimajor, a, and semiminor, b, axes of the individual trellis contact patches, using the formulations presented by Raoof (1990b).
4. Use (19)–(20e) to calculate σ_x, assuming μ = 0.12 (Raoof 1990c).
5. Calculate the value of trellis contact patch spacing, x, by (14).
6. Use (4) and (16)–(17b) with the appropriate values of the parameter u to calculate the magnitude of interwire-interlayer slippage at the critical location.
7. Calculate $S = \sigma_x U/x$, and hence, read off the expected free-bending fatigue life from the plot in Fig. 3.

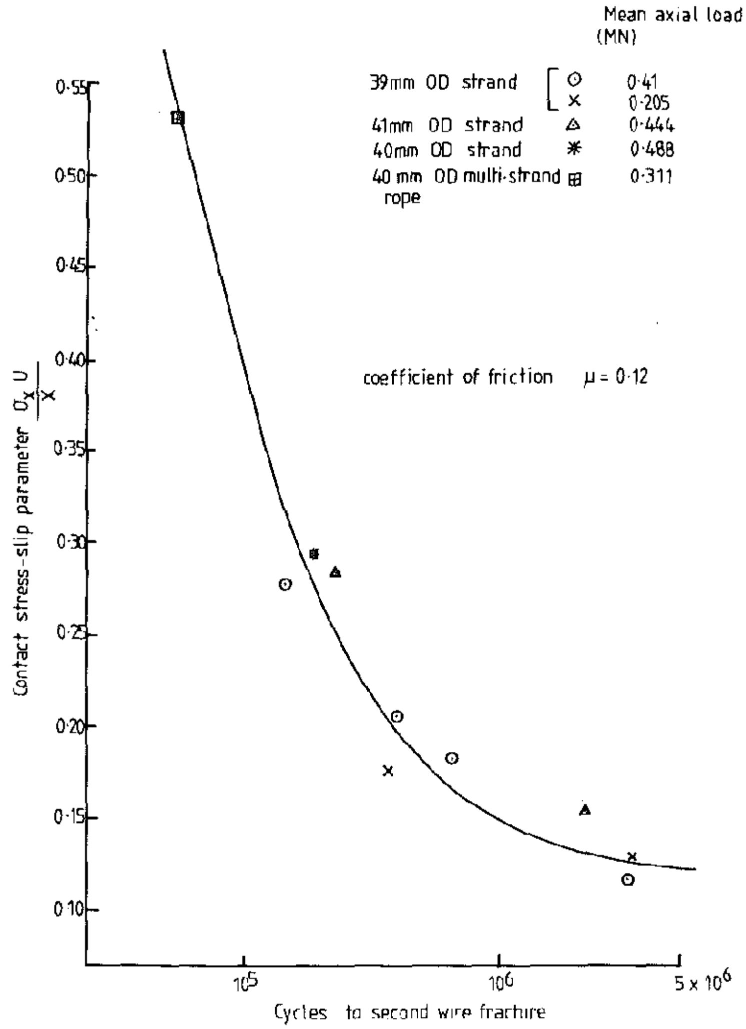

FIG. 3. Relationship between Contact Stress-Slip Parameter, S, and Free-Bending Fatigue Life for Spiral Strand

Effect of Hydrostatic Pressure on Sheathed Strands

High-density, supposedly impermeable polyethylene sheaths have been offered by cable manufacturers for corrosion protection of large-diameter spiral strands used in deep-water applications. Under such conditions, Raoof (1990a) has shown that the clench forces due to the hydrostatic water may become significant compared with the clench forces inside the spiral strand caused by the axial load in, say, a guyed tower or communications and power cable applications. In other words, with high hydrostatic pressure on a sealed electromechanical cable with soft cores or gas-filled voids, the presence of substantial air-filled voids in the sheathed cable will ensure that the wires will experience some extra clench forces.

Under these conditions, extensive numerical studies have shown that the value of interlayer relative slippage, U, for spiral strands under free-bending conditions, is, for all practical purposes, independent of the level of external pressure. This is mainly due to the rather small variations of the shear interwire stiffness, K_1, with the potential variations in the level of interwire contact forces. However, σ_x is found to be a nonlinear function of water depth (Fig. 4). In this figure, σ_x is plotted for the trellis contact patches between the outer and penultimate layers of a 39-mm-OD spiral strand [with construction details given by Raoof (1990a) elsewhere], subjected to various levels of imposed mean axial load.

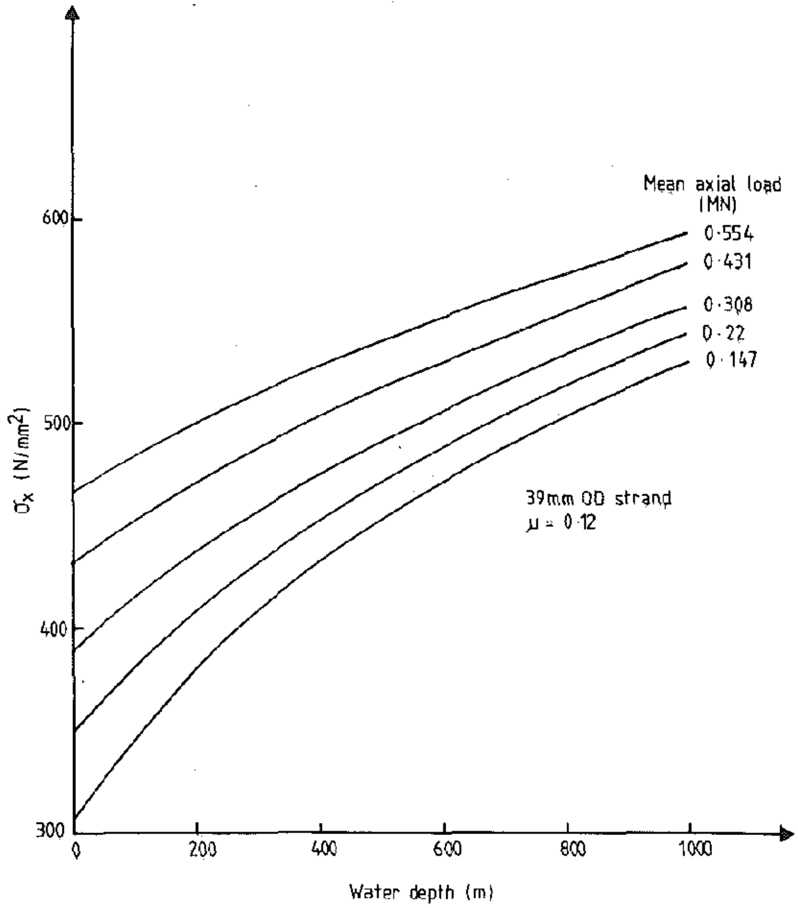

FIG. 4. Variation of Alternating Component of Tensile Stress, σ_x, at Trailing Edge of Trellis Contact Patch with Level of Strand Mean Axial Load and Level of External Hydrostatic Pressure on Sheathed 39-mm-OD Strand

Data in Fig. 4 in conjunction with the $\sigma_x U/x$ against fatigue life plot of Fig. 3 may then be used to construct contact stress-slip parameter versus fatigue cycles fatigue curves for the sealed 39-mm-OD strand subjected to various levels of external water depth (Fig. 5).

In these figures, the ordinates have been normalized to ease comparison of the results. This has been achieved by dividing $\sigma_x U/x$ by K', where

$$K' = \frac{\sigma_x \text{ (given water depth)}}{\sigma_x \text{ (zero water depth)}} \quad \text{(22)}$$

Thus, at a water depth of 1,000 m, and assuming a mean load of 0.197 MN, Fig. 4 gives $K' = 530/308 = 1.72$.

Curve A in Fig. 5(a) (in air data) gives a fatigue life of 10^6 cycles at $\sigma_x U/x = 0.145$. For 1,000 m of water depth, then, $\sigma_x U/x = 1.72 \times 0.145 = 0.2495$, which gives a fatigue life from curve A of 1.584×10^5 cycles, which is a very significant reduction from 10^6 cycles. Alternatively, curve B (corresponding to 1,000 m of water) may be used to obtain the same fatigue life of 1.584×10^5 cycles corresponding to $\sigma_x U/(K'x) = 0.145$.

Figs. 5(a) and 5(b) demonstrate that the effect of water pressure on strand free-bending fatigue life increases with decreasing strand mean axial load.

The substantial reductions in strand free-bending fatigue life may have a significant bearing on the estimated operational life span of the moored system. Such effects have invariably been ignored in previous designs of sealed terminations in, for example, guyed-tower platform applications.

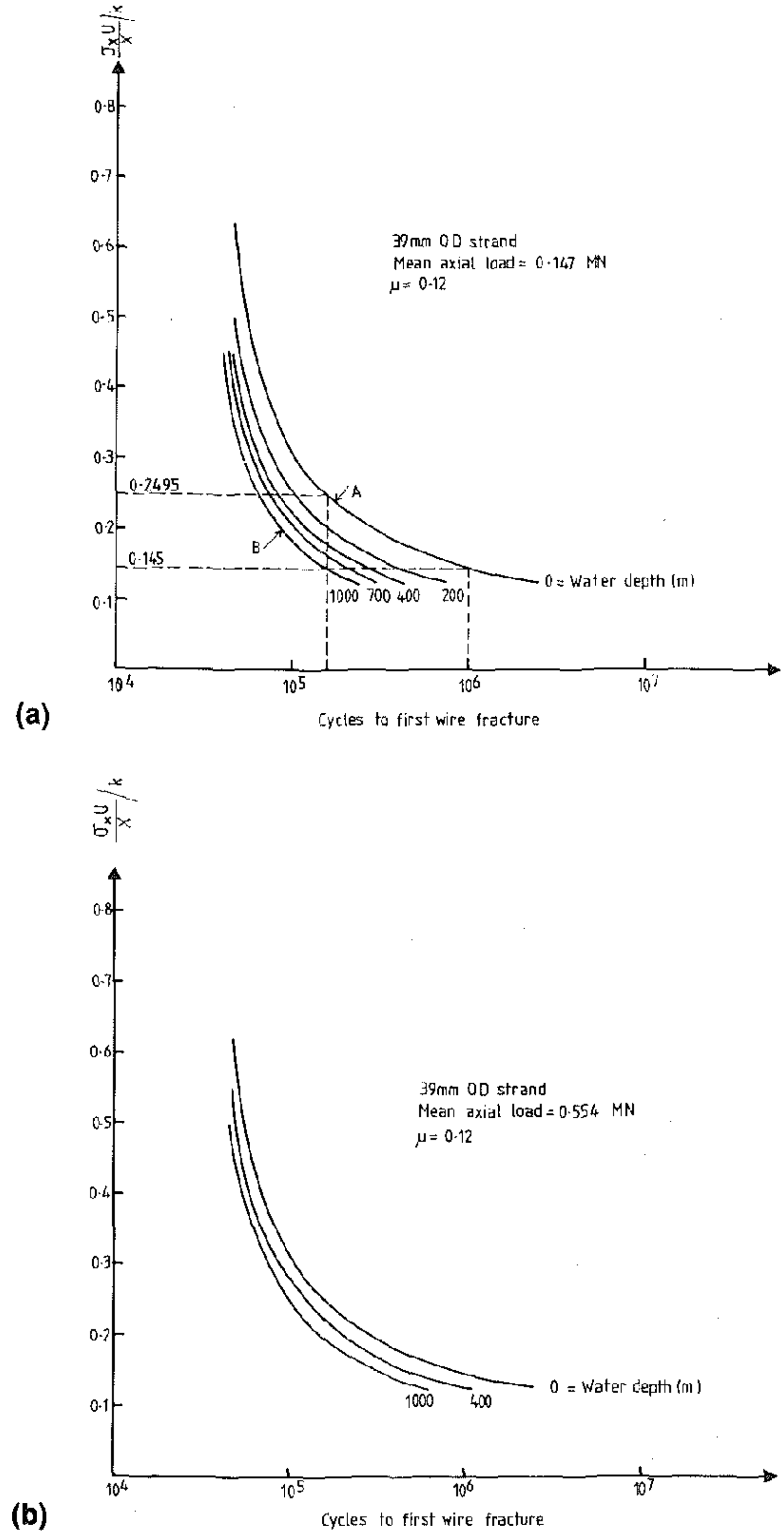

FIG. 5. Variation of Sheathed Strand Free-Bending Fatigue Life as Function of External Hydrostatic Pressure: (*a*) Mean Axial Load = 0.147 MN; (*b*) Mean Axial Load = 0.554 MN

Multistrand Ropes

Multistrand ropes are composed of a helical assembly of a number of seven wire strands in a number of concentric layers around a central (straight) core: Fig. 6 gives two representative examples of such constructions offered by cable manufacturers.

The approach adopted here for the free bending fatigue analysis of mul-

FIG. 6. Examples of Multistrand Rope Constructions

TABLE 1. Construction Details for 40-mm-OD Multistrand Rope

	Strand Distribution in Rope		Details of Individual Seven-Wire Strands			
Layer in rope i (1)	Number of strands m (2)	Lay angle β (degrees) (3)	Layer in strand (4)	Number of wires n (5)	Wire diameter D (mm) (6)	Lay angle α (degrees) (7)
core (1)	1	0	core (1)	1	1.8	0
king strand			2	6	1.7	−12.28
2	5	−19.85	core (1)	1	1.8	0
			2	6	1.65	+12.18
3	11	−19.97	core (1)	1	1.7	0
			2	6	1.6	−12.07
4	17	−20.02	core (1)	1	1.6	0
			2	6	1.5	+12.06
5	23	+20.02	core (1)	1	1.55	0
			2	6	1.45	−11.88

tistrand ropes is similar to that adopted for the analysis of spiral strands. Table 1 gives construction details for the 40-mm-OD multistrand rope, whose free-bending fatigue life is reported by Strezemiecki and Hobbs (1988): they found the failure of the individual (seven-wire) strands in the multistrand rope experiencing cyclic free bending to initially happen in the vicinity of the so-called neutral axis at the fixed socket where the imposed radius of curvature was greatest. In the case of multistrand ropes, the size of the individual strands is rather small, with a large number of them in various layers. The proposed method of free-bending analysis is to treat the individual strands as wires assembled in spiral strand. Consequently, the analysis for free-bending maximum interwire slippage may be treated as before, with the proviso that an alternative method should be developed for estimating the value of no-slip shear stiffness, K_{1n}. Due to the rather complex pattern of interwire contact between various seven-wire strands, exact determination of K_{1n} using available contact stress theories is fraught with difficulties. However, numerical results on the trellis contact of individual wires in spiral strands covering the practical range of manufacturers' current limits, suggest that the value of K_{1n} for the operational ranges of mean axial loads may be reasonably given by the plot in Fig. 7. In this figure, it is shown that for current ranges of lay angles, $11° < \alpha < 25°$, and wire diameters, for some

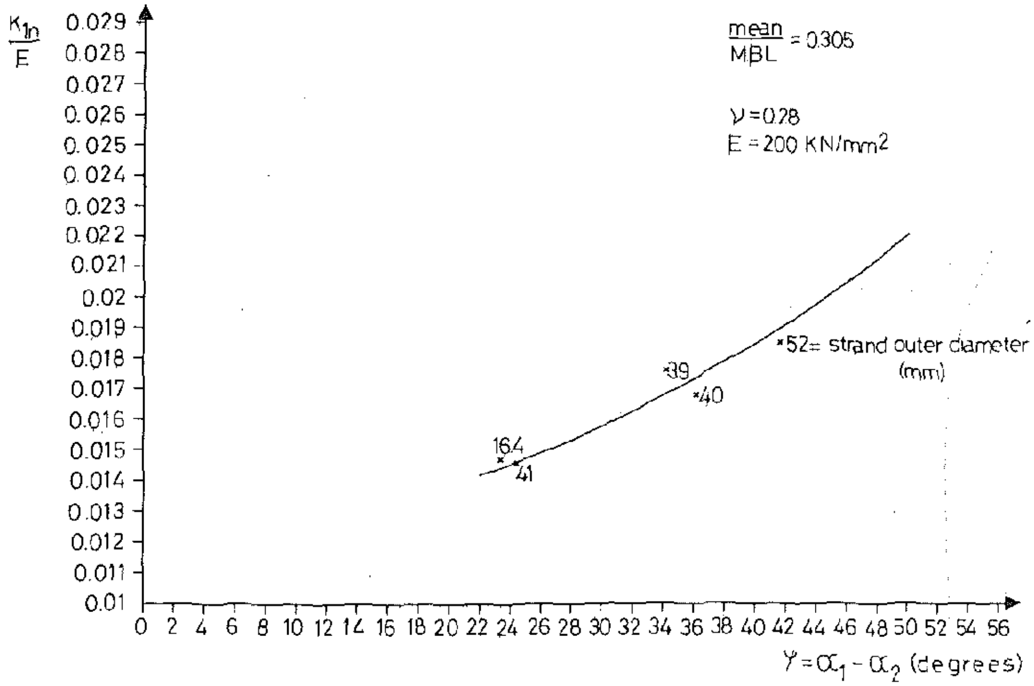

FIG. 7. Variation of No-Slip Secant Shear Stiffness, K_{1n}, with Total Angle between Outer and Penultimate Layers of Multistrand Ropes

representative spiral strands, the magnitude of K_{1n} assumed to be given as the value of the nondimensionalized shear stiffness along the major principal axis of the elliptic contact patches may reasonably be presented by a single curve as a function of the total angle between the outer and penultimate layers (1 and 2). For the present purposes, it is suggested that a reasonable estimate of K_{1n} for multistrand ropes, under average working mean axial loads, may be obtained from the plot in Fig. 7, with the proviso that the lay angles α_1 and α_2 represent the lay angles of the seven wire strands in the rope's outer and penultimate layers, respectively. It must be emphasized that numerical studies on spiral strands suggest that a reasonable (nevertheless approximate) estimate of K_{1n} is sufficient for obtaining fairly accurate estimates of maximum interwire-interlayer slippage, U.

Fig. 8 presents variations of the parameter σ_x for a wide range of strand constructions (Table 2), as a function of the total angle between wires in the outer and penultimate layers. The assumed mean axial load on the strands is 30.5% of their maximum breaking load. Over the practical range of lay angles, $11° < \alpha < 25°$, values of σ_x appear to be very nearly constant, irrespective of strand construction details.

The pattern of interlayer contact patches between the outer and penultimate layers in a multistrand rope may be assumed to behave similarly to the contact between two bearing surfaces occurring at the tips of their surface asperities. Hertzian normal contact theory has in the past been extensively applied to such problems and is supported by a rather large body of literature on the topic. It is shown that frictional behavior is dominated by the properties of these small regions of contact, which, under cyclic loading, may be assumed to behave elastically (Archard 1957). For the present purposes, it will be assumed that a constant value of σ_x as given by the asymptotic solution to the plots of σ_x versus ψ, which depends on the level of strand axial preload, may be used for the estimation of the appropriate value of σ_x to be used in estimates of contact stress-slip parameter. Such an approach has been adopted for analyzing the free-bending fatigue behavior of the 40-

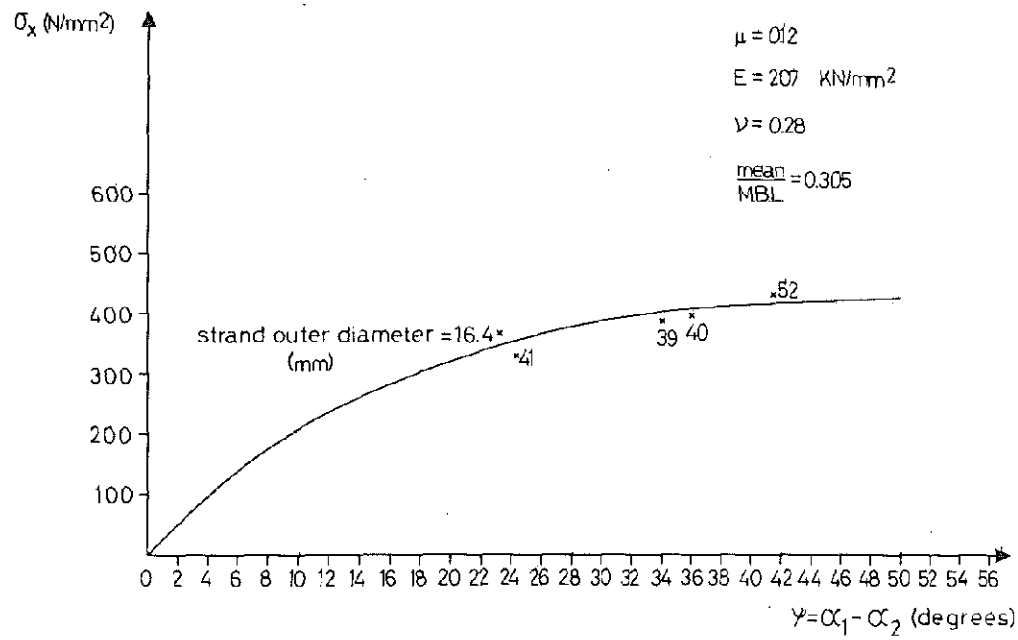

FIG. 8. Variation of σ_x with Total Angle between Outer and Penultimate Layers of Multistrand Ropes—Mean Axial Load/Maximum Breaking Load = 0.305

TABLE 2. Construction Details For Spiral Strands used in Parametric Study

Strand outer diameter (nominal) (mm) (1)	Outer Layer			Penultimate Layer		
	α_1 (degrees) (2)	n_1 (3)	D (mm) (4)	α_2 (degrees) (5)	n_2 (6)	D (mm) (7)
16.4	11.91	12	3.25	−11.42	6	3.25
39	17.74	30	3.54	−16.45	24	3.54
40	18.07	54	2.08	−18.07	48	2.08
41	12.45	24	4.57	−11.96	18	4.57
52	20.93	42	3.38	−20.68	36	3.38

mm-OD multistrand rope, and the result is presented in Fig. 3, the correlation with the other data on various spiral strand constructions is found to be satisfactory. It is suggested that the plot in Fig. 3 may be used for estimating the free-bending fatigue life of both spiral strands and multistrand ropes. The limited nature of publicly available (and reliable) experimental data used for obtaining the plot in Fig. 3 must, however, be borne in mind until more test data on other cable constructions become available.

Conclusions

Using a simplified version of some previously reported analytical models, the magnitude of maximum interwire-interlayer slippage between outer and penultimate layers of an axially preloaded spiral strand, undergoing free bending with its end clamped, has been developed. Using such information in conjunction with well-established results in the field of contact stress theory, a parameter has been suggested for estimating the free-bending fatigue life of strands whose initial wire fractures invariably occur near the fixed terminations. Following some previously reported experimental observations on a number of substantial spiral strands, the proposed theory assumes interwire-interlayer fretting to be the main mechanism for wire fractures under cyclic loading. This is in direct contrast to previously available research, which invariably has used the direct stresses in the extreme fiber position (in terms of simple beam-bending theory), to estimate strand free-bending fatigue performance. The proposed model takes interwire friction fully into account, and in line with experimental observations, identifies the location in the vicinity of the so-called neutral axis, where wires enter the socket, as the critical place for initial wire breakages.

The theory also demonstrates the possibility of substantial reductions in sheathed strand free-bending fatigue life in deep-water applications, which may have significant bearing on the estimated operational life span of moored systems in, say, a guyed-tower platform application. Previously, deep-water–platform designers have invariably ignored such effects.

By employing some reasonable simplifying assumptions, it has also been possible to offer a similar parameter for estimating free-bending fatigue life of multistrand ropes in the vicinity of end terminations.

Acknowledgments

The writer acknowledges the long-standing and friendly cooperation of Bridon Ropes' personnel at Doncaster. The writer is also grateful to R. E. Hobbs, of Imperial College, London, for vaious stimulating discussions in the initial stages of this research. Finally, thanks are due to Ada Lam for typing the manuscript.

Appendix I. References

Archard, J. F. (1957). "Elastic deformation and the laws of friction." *Proc. Royal Soc. London*, A243, 190–205.

Costello, G. A., and Buston, G. J. (1982). "Simplified bending theory for wire rope." *J. Engrg. Mech.*, ASCE, 108(4), 219–227.

Hobbs, R. E., and Ghavami, K. (1982). "The fatigue of structural wire strands." *Int. J. Fatigue*, 4, Apr., 69–72.

Hobbs, R. E., and Smith, B. W. (1983). "The fatigue performance of socketed terminations to structural strands." *Proc. Inst. Civ. Engrs.*, Part 2, 25, Mar., 35–48.

Jahnke, E., and Emde, F. (1945). *Tables of functions*. Dover Publications Inc., New York, N.Y.

Johnson, K. L., and O'Connor, J. J. (1963). "Mechanics of fretting." *Proc. Appl. Mech. Convention*, Inst. Mech. Engineers, 178, Part 3J., 7–21.

Knapp, R. H. (1988). "Helical wire stresses in bent cables." *J. Offshore Mech. Arctic Engrg. Trans. ASME*, 110, Feb., 55–61.

Lutchansky, M. (1969). "Axial stresses in armour wires of bent submarine cables." *J. Engrg. Ind. Trans. ASME*, 91, Aug., 687–693.

Nowak, G. (1974). "Computer design of electromechanical cables in ocean applications." *Proc. 10th Annual MTS Conf.*, Washington, D.C., 293–305.

Phillips, J. W., Miller, R. E., and Costello, G. A. (1980). "Contact stresses in a straight cross-lay wire rope." *First Annual Wire Rope Conf.*, Denver, Co., Mar., 177–200.

Poffenberger, J. C., and Swart, R. L. (1965). "Differential displacement and dynamic conductor strain." *IEEE Trans. Power Apparatus Systems*, PAS-84, Apr., 281–289.

Raoof, M., and Hobbs, R. E. (1984). "The bending of spiral strand and armoured cables close to terminations." *J. Energy Resour. Tech. Trans. ASME*, 106, Sep., 349–355.

Raoof, M., and Hobbs, R. E. (1988). "The analysis of multilayered structural strands." *J. Engrg. Mech.*, ASCE, 114(7), 1166–1182.
Raoof, M., and Hobbs, R. E. (1989). "The tangential compliance of rough elastic bodies in contact." *J. Trib. Trans. ASME*, 111, Oct., 726–729.
Raoof, M. (1989). "Free bending tests on large spiral strands." *Proc. Inst. Civ. Engrs.*, Part 2, 87, Dec., 605–626.
Raoof, M. (1990a). "Effect of hydrostatic pressure on strand behaviour." *J. Strain Anal.*, 25(2), 75–84.
Raoof, M. (1990b). "Free bending of spiral strands." *J. Engrg. Mech.*, ASCE, 116(3), 512–530.
Raoof, M. (1990c). "A multicontact problem." *Proc. Ninth Int. Conf. Exp. Mech.*, Technical University of Denmark, Lyngby, Denmark, Aug., 103–111.
Raoof, M. (1990d). "Axial fatigue of multi-layered strands." *J. Engrg. Mech.*, ASCE, 116(10), 2083–2099.
Raoof, M. (1990e). "Axial fatigue life prediction of structural cables from first principles." *Proc. Inst. Civ. Engrs.*, Part 2, 91, Mar., 19–38.
Raoof, M., and Huang, Y. P. (1992). "Wire stress calculations in helical strands undergoing bending." *J. Offshore Mech. Arctic Engrg.*, (in press).
Raoof, M. (1992). "Axial fatigue prediction for structural cables." *The Structural Engineer* (in press).
Richardson, A. S. (1989). "Paradox unresolved." *J. Engrg. Mech.*, ASCE, 115(5), 905–912.
"Standardization of conductor vibration measurements." (1965). *Paper 31 TP 65-156*, Winter Power Meeting, Jan., IEEE, New York, N.Y.
Strzemiecki, J., and Hobbs, R. E. (1988). "Properties of wire ropes under various fatigue loadings." *CESLIC Report SC6*, Sep., Dept. of Civil Engineering, Imperial College, London, U.K.
Vermeulen, P. J., and Johnson, K. L. (1964). "Contact of non-spherical elastic bodies transmitting tangential forces." *J. Appl. Mech. Trans. ASME*, 31, 338–340.
Webster, S. E., Rudd, W. J., and Cook, W. T. (1982). "Review of information on the fatigue of tethering systems for tethered buoyant platforms." BSC Research Services, U.K. Department of Energy, London, U.K.

Appendix II. Notations

The following symbols are used in this paper:

- A = wire cross-section area;
- a = semi-axis of elliptic contact patch parallel to applied tangential force, semimajor axis;
- B = complete elliptic integral;
- b = semi-axis of elliptic contact patch perpendicular to direction of applied tangential force, semiminor axis;
- C = complete elliptic integral = $(2D - K)/k_1^2$;
- c = $\sqrt{(r_1 - r_w)^2 + k^2}$;
- D = complete elliptic integral = $(K - E)/k_1^2$, wire diameter;
- E = Young's modulus;
- G = shear modulus = $E/[2(1 + \nu)]$;
- K = complete elliptic integral;
- K_1 = interwire-interlayer secant shear stiffness;
- K_{1f} = full-slip interwire-interlayer secant shear stiffness;
- K_{1n} = no-slip interwire-interlayer secant shear stiffness;
- K' = σ_x (given water depth) divided by σ_x (zero water depth);
- k, k_1 = modulus of elliptic integrals;
- N = wire tensile force;

n_2 = number of wires in second layer of spiral strand;
P_R = total normal force of elliptic interlayer contact patch;
r_1 = helix radius in outer layer of spiral strand;
r_w = wire radius;
S = contact stress-slip parameter = $\sigma_x U/x$;
s_c = coordinate along helical wire;
T = tangential force;
U = maximum magnitude of interlayer slippage in vicinity of neutral axis;
u = wire axial movement;
u^p = underlying core displacement;
x = spacing between trellis contact patches along outer wire (or outer seven-wire strand) of spiral strand (or multistrand rope);
α_1, α_2 = lay angles in outer and penultimate layers of spiral strands and multistrand ropes;
δ_t = tangential displacement per two bodies in contact;
$\delta_{t\max}$ = tangential displacement between two bodies in contact at onset of full sliding when $T = \mu P_R$;
θ = polar angle of helical wire;
θ_0 = helix polar angle (always negative) at which toroidal section starts (i.e., at clamp);
$\theta_0^{\max}$ = polar angle at clamp where highest wire axial strain takes place (always negative);
μ = coefficient of friction;
ν = Poisson ratio;
ρ = radius of curvature;
σ_x = maximum magnitude of alternating component of tensile stress at trailing edge of elliptic contact patch parallel to direction of applied tangential force; and
ψ = total angle between outer and penultimate layers (layers 1 and 2) in spiral strand or multistrand rope.